SIDESTREAM OPTIMIZATION THROUGH THE USE OF COMPUTATIONAL FLUID DYNAMICS AND MODEL TESTING

by

James M. Sorokes

Team Leader, Aero-Performance Group

David A. Nye

Senior Analysis Engineer

Dresser-Rand Olean Operations

Olean, New York

Nicholas D'Orsi

Associate Head of Engineering Design and Development

Concepts ETI, Inc.

Wilder, Vermont

and

Rob Broberg

Team Leader, Applications

AEA Technology/Advanced Scientific Computing

Waterloo, Ontario, Canada

James M. Sorokes has been employed at Dresser-Rand (formerly Dresser-Clark) for 24 years, all of those in the Aerodynamics Group, in Olean, New York. He has held various supervisory positions since 1984 and is currently the team leader of the Applied Aerodynamics Group. In this capacity, he is responsible for the development, design, and analysis of all rotating and stationary aerodynamic components of centrifugal compressors. Specific areas of concentration include single stage rig testing, aeromechanical phenomenon (i.e., rotating stall), practical application of CFD, alternate design philosophies and techniques, etc.

Mr. Sorokes received a B.S. degree from St. Bonaventure University (1976). He is a member of AIAA, ASME, and the ASME Turbomachinery Committee. He has authored or coauthored more than 20 technical papers and has been an instructor at various seminars and tutorials at Texas A&M University and Dresser-Rand. He also holds two U.S. patents.

David A. Nye is currently employed as a Senior Analysis Engineer in the Aero-Performance Group at Dresser-Rand, in Olean, New York. He has held several technical positions at Dresser-Rand in the centrifugal compressor and gas turbine areas. Prior to joining Dresser-Rand, he was employed by Allison Engine Company, in Indianapolis, Indiana, as a Senior Combustion Engineer involved in the design of low emission gas turbine fuel injectors.

Dr. Nye received his Ph.D. degree (Mechanical Engineering/Combustion, 1993) from The Pennsylvania State University after receiving a B.S. degree (Mechanical Engineering, 1988) from Clarkson University.

Nicholas D'Orsi is the Associate Head of Engineering Design and Development at Concepts ETI, Inc. (CETI), in Wilder, Vermont. Since arriving at CETI in 1991, he has been actively involved in the fluid dynamic and structural design and analysis of all types of turbomachinery components, including axial, radial, and mixed-flow compressors, turbines, and pumps. Mr. D'Orsi has been the lead engineer in numerous turbomachinery projects, includ-ing CETI's consortia and a large number of compressor and rocket turbopump design and test projects. Before joining CETI, he worked at Textron Lycoming (now AlliedSignal), in Stratford, Connecticut, as a Development Engineer, analyzing thermo-dynamic cycles of advanced gas turbine engines and developing preliminary designs for gas turbine compressors and turbines.

Mr. D'Orsi received B.S. and M.S. degrees (Aeronautical Engineering) from Rensselaer Polytechnic Institute. He is a member of ASME and serves on the board of the ASME Process Industries Division.

ABSTRACT

The development of sidestreams for industrial centrifugal compressors presents many difficult challenges for aerodynamic designers. Most often, past practice dictated the configurations used for new applications. However, as end user's demanded higher performance and improved predictability, better design methodologies had to be developed.

More effective use of computational fluid dynamics (CFD) codes was an obvious solution. However, to properly use such codes, they must be calibrated or validated against available test data. To this end, the OEM funded an extensive project combining model testing with detailed CFD analyses. The goal was to establish more rigorous design and analysis guidelines for incoming sidestreams.

Under the project, two sidestream configurations were model tested and analyzed. The test rig, instrumentation, and test program are described in detail. Comparisons are made between the measured data and CFD results. Comments are offered regarding the agreement in the experimental and computational results. Similarities between the model test results and those obtained from a production compressor are also discussed. Finally, observations are presented relative to the use of CFD as a sidestream design tool.

INTRODUCTION

One of the most complex turbomachines used in the process industry is the sidestream compressor. Sidestream compressors are characterized by their multiple flanges at which flow is either added or removed as required by the end users' process. That is, flow enters or leaves the machine at other than the main inlet or main discharge. Sidestream compressors play an important role in the processing of heavy hydrocarbons; i.e., propane, propylene, methyl tert-butyl ether (MTBE), etc. While such machines often employ both incoming and outgoing sidestreams, this work addresses incoming sidestreams only as they are the more common of the two types.

Before proceeding further, some terminology must be defined to ease the remainder of the discussion. *Core flow* will refer to that portion of the process flow that is already in the compressor prior to the injection of the *sidestream flow*. *Sidestream flow* will then refer to the additional flow that enters the machine through the sidestream flange. The term *mixed flow* will be used when addressing the combined sidestream and core flows.

What makes sidestream design difficult is that flows entering the machine must be mixed with the core flow already in the machine in such a manner so as to not degrade the aerodynamic performance of the surrounding compressor staging. Effective sidestream performance can only be attained by minimizing losses in the sidestream itself while also achieving good mixing of the core and sidestream flows prior to their injection into the downstream impeller. Of course, the designer must accomplish this aerodynamic mixing without adding significant axial length or else the compressor will become unacceptable rotordynamically.

Adding to the complexity, the end user's process dictates the pressure at which the flow must be injected. Therefore, the staging upstream of the sidestream must achieve the necessary static pressure ratio such that the core flow is at the required pressure at the sidestream mixing section. Further, the incoming flows are typically at a temperature different from that of the compressor core flow stream. Designers must be cognizant of the possible detrimental influences of temperature stratification on the downstream impellers. Finally, it is commonplace for a propane or propylene machine to have as many as three sidestreams. In short, there are many concerns that must be addressed when developing an effective sidestream.

Incoming sidestreams take on a variety of configurations. However, the most common arrangement used in process compressors looks similar to that shown in Figure 1. Flow enters the compressor through an inlet nozzle and is distributed around the circumference of the machine via a plenum chamber. Flow then passes through a scoop or deswirl vane cascade where it merges in the downstream guidevane with the core flow exiting the adjacent return channel.

Historically, sidestreams have been designed using simple bulk flow techniques. Compressor vendors, through experience, trial, and error, discovered a configuration that provided acceptable performance. However, difficulties were often encountered when faced with applications that fell outside prior experience. The only option in this situation was to "cut and try" until a successful alternate was found.

More recently, end users have begun to demand more and more stringent tolerances on sidestream pressure levels. In addition, they are specifying more than one required operating (or guarantee)
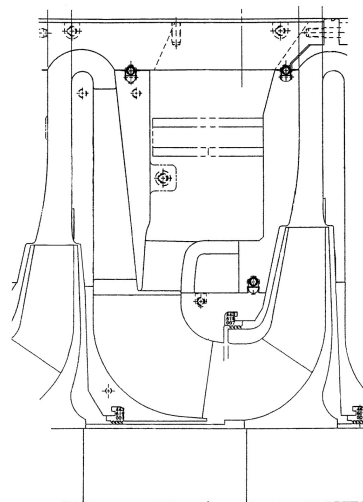

Figure 1. Typical Sidestream Cross-Section.

condition. Even further, the flow requirements of many new plants are forcing OEM's into compressors with much higher tip and inlet relative Mach numbers (U2/A0 and Mrel1t, respectively). All these factors are driving OEM's to seek more accurate analytical and prediction systems.

With advances in computational fluid dynamics (CFD), it has become possible to analyze the complicated geometries and complex flow fields associated with sidestreams. These detailed analyses allow the study of flow behavior in the various passage of the sidestream as well as the effects of the sidestream exiting flow on downstream components; i.e., the impeller. Flow physics contributing to excess losses can be identified and alternate configurations can be assessed prior to building any equipment.

The CFD software developer referred to in this paper is AEA Technology/Advanced Scientific Computing. For all CFD simulations in this study, the CFX-TASCflow Version 2.9 (1999) computational fluid dynamics software was employed.

In this investigation, a number of CFD analyses were conducted on an initial and several alternate sidestream configurations. It should be noted that the configurations analyzed did not conform to any specific sidestream design used by the OEM, but rather captured the general arrangement employed (again, refer to Figure 1). The computational domain included the return channel, the entire sidestream, and the downstream inlet guidevane. Runs were completed at various core flow to sidestream flow ratios to simulate those encountered in a typical sidestream machine. In addition, different temperatures were used for the sidestream and core flows to determine if temperature stratification influences the performance of the downstream impeller.

To gain confidence in the solutions they provide, CFD analyses must be calibrated against high quality test data. Some attempts were made in the past to gather these data during production testing. One example will be presented later. However, it is typically very difficult to get enough instrumentation into a customer's unit to allow a detailed assessment of the losses through the sidestream passages. Therefore, as part of the development effort, a sidestream model test rig was constructed at an independent researcher's facility, Concepts ETI, Inc. The rig was constructed to maximize visual access to the various flow passages including the return channel, sidestream plenum, scoop vane, and downstream inlet guidevane area. Pressure and temperature traversing were done at various locations within the model and numerous stationary probes were installed. In addition, tufts were used to assist in flow visualization. Like the CFD analyses, various flow ratios and differing temperatures (core to sidestream) were tested so that measured data could be compared with the analytical results.

The data obtained and trends observed in the model testing were compared against the CFD results, and conclusions were drawn regarding the value of each in the development of sidestreams.

THE MODEL TEST RIG

Given the size of a typical sidestream machine, it was cost prohibitive to do the research testing on a full-scale compressor. In addition, getting the information necessary to validate or calibrate the CFD models would be difficult during a production test. Further, flow visualization would be required to search for phenomena (i.e., swirl cells, separations, etc.) within the various elements of the sidestream. Visual access to the various flow passages would be required; again, difficult in a production machine. Therefore, it was decided to develop a model test vehicle.

Since the OEM has limited experience developing such rigs, a decision was made to work with an outside resource, an independent research facility. An agreement was forged and the outside resource assembled the test rig based on design guidelines provided by the OEM. Discussions were also held to establish the instrumentation and operating requirements.

An experimental rig to simulate a typical industrial sidestream device was designed, fabricated, and tested at the independent researcher's facility for the OEM. This rig modeled the two flows present in a sidestream device: the core flow, which is the main compressor throughflow, and the sidestream flow, which is injected into the flow path at some point downstream of the impeller discharge. This rig was designed to pass anywhere from zero percent sidestream flow to equal amounts of core and sidestream flow. Two variations on this test rig were fabricated and tested. The first, designated original build, used a constant area plenum and straight vanes in the sidestream flow side. An assembly drawing of the original build sidestream test rig can be seen in Figure 2. The second, designated modified build, used a plenum with a "walk plate" and "scoop" vanes in the sidestream flow side. The walk plate is used to vary the sidestream plenum area around the circumference. The plenum area is greatest at the location the sidestream flow enters the plenum and smallest opposite this location. The scoop vanes are used to improve the sidestream device performance by reducing the flow incidence onto the sidestream guidevanes. An assembly drawing of the modified build sidestream test rig is shown in Figure 3. An axial view of the straight vanes and scoop vanes can be seen in Figure 4. A photograph of the original build test rig is shown in Figure 5.
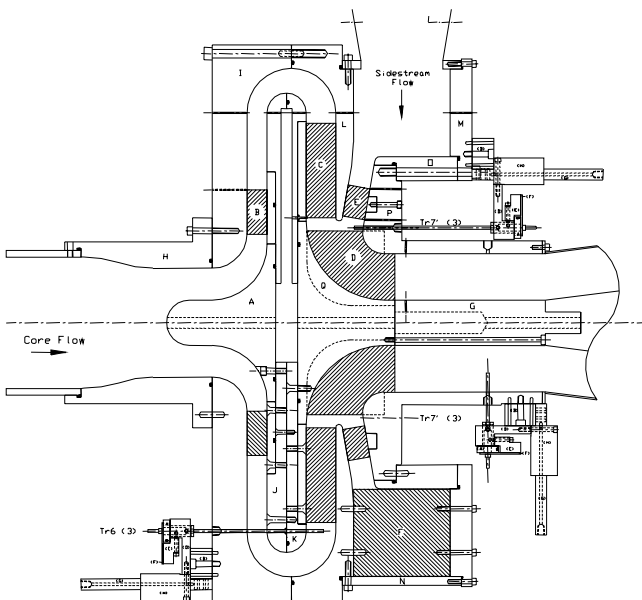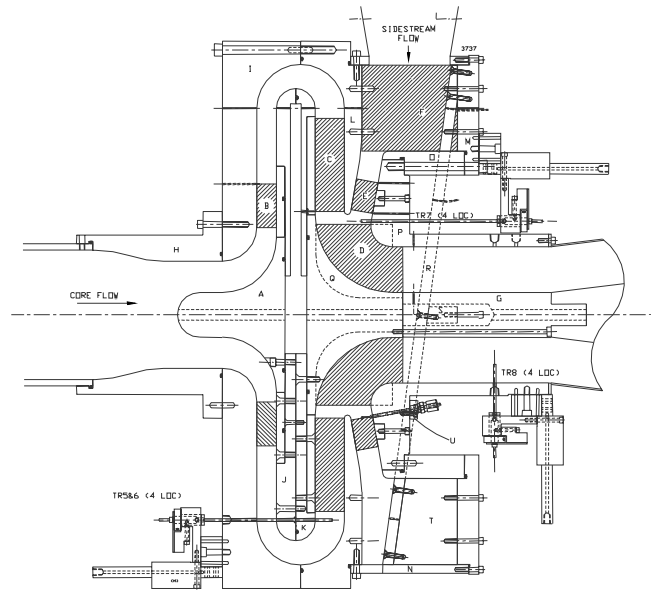

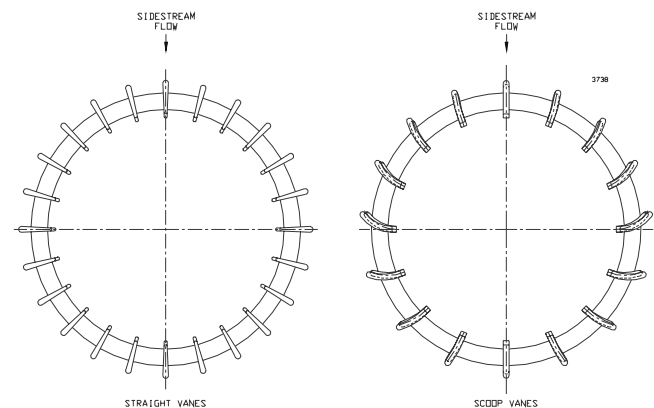*Figure 3. Sidestream Test Rig Assembly Drawing, Modified Build.*

Figure 4. Two Types Sidestream Guidevanes, Straight Vanes and Scoop Vanes.
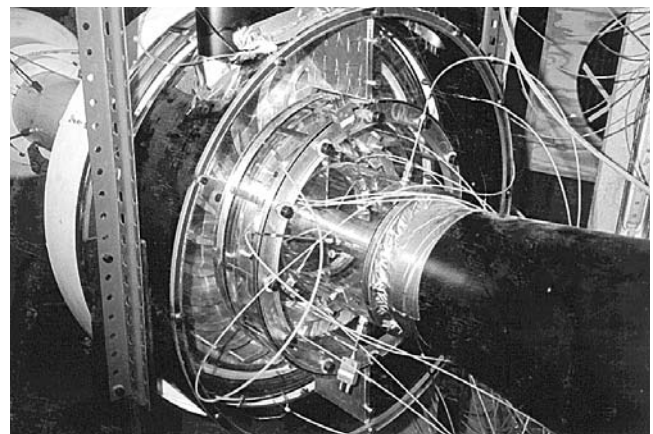

Figure 5. Photograph of Sidestream Test Rig.

Looking at Figure 2, the core flow enters the rig through an ASME bellmouth, goes around a 90 degree bend formed by the inlet centerbody (A) and outer return bend front plate (I), passes through a preswirl cascade (B) that simulates the impeller by inducing swirling flow, goes outward through a parallel wall

Figure 2. Sidestream Test Rig Assembly Drawing, Original Build.

vaneless diffuser, flows around a 180 degree bend and through a set of radial deswirl vanes (C). The 180 degree bend and radial deswirl vanes simulate a typical industrial return channel (diaphragm). At the exit of these radial deswirl vanes, the core flow mixes with the sidestream flow as it passes through a set of exit guidevanes (D), around a 90 degree bend, and exits the test rig.

The sidestream flow passes through a bellmouth, enters a circular inlet pipe that transitions into an oval pipe, and flows into a sidestream plenum formed by the sidestream plenum back plate (M), sidestream plenum inner ring (O), and outer return bend back plate (L). This plenum has splitters at zero degrees (oval pipe inlet) and 180 degrees to prevent the sidestream flow from circling the plenum. From the sidestream plenum, the flow passes through a set of sidestream guidevanes (E), and then mixes with the core flow as it passes through the exit guidevanes (D) and exits the rig.

This test rig was fabricated out of steel, aluminum, epoxy, and Plexiglas. The Plexiglas was used in key locations to allow flow visualization with fixed tufts and traversing wands. The Plexiglas pieces are the outer return bend back plate (L), sidestream plenum back plate (M), sidestream inner ring (O), and guidevane back plate (P). Fixed tufts were attached throughout the return channel, sidestream plenum, sidestream splitters, sidestream guidevanes, and exit guidevanes. Traversing wands with attached tufts were used at the return channel guidevanes inlet, in the region where the core and sidestream flow mixed, and throughout the exit guidevanes and stage exit. The test rig was heavily instrumented with both fixed and traversing pressure and temperature instrumentation. For original build, there were 63 fixed pressure measurements taken at each operating point, nine of these were total pressures measured using Kiel probes, and the remaining 54 were 0.020 inch diameter wall static pressure taps. In addition to these fixed pressure measurements, there were 14 locations for full flowfield traversing (total pressure, static pressure, flow angle, total temperature) using three-hole cobra probes and half-shielded thermocouples, and 10 fixed half-shielded thermocouples for total temperature measurement. A summary of the instrumentation at each location for original build is contained in Table 1. The instrumentation for the modified build was slightly different from that of original build. A summary of the modified build instrumentation can be found in Table 2.

Table 1. Sidestream Test Rig Instrumentation, Original Build.

Location	Instrumentation
Core	
Inlet	3 total pressures, 3 static pressures, 3 total temperatures
Preswirl cascade exit	4 static pressures
Vaneless diffuser exit	8 static pressures, 4 traverse locations
Radial deswirl cascade inlet	8 static pressures, 4 traverse locations
Radial deswirl cascade exit	8 static pressures, 3 traverse locations
Sidestream	
Inlet	3 total pressures, 3 static pressures, 3 total temperatures
Plenum	4 static pressures
Guide vane inlet	4 static pressures
Guide vane exit	4 static pressures, 3 traverse locations (same as core deswirl exit)
Stage Exit	3 total pressures, 8 static pressures, 4 total temperatures

A blower driven by a 75 hp electric motor provided airflow for the sidestream test rig. The air is pulled through the sidestream test rig from ambient conditions at the core inlet to a slightly subatmospheric condition at the rig exit. The capacity of this blower is set by a number of factors, including the losses through the test device. The maximum airflow for the testing reported in this paper was about 6.5 lbm/s (3.25 lbm/s core and 3.25 lbm/s sidestream), or 5100 scfm. Total airflow through the system was controlled by a butterfly valve at the blower inlet. The core flow

Table 2. Sidestream Test Rig Instrumentation, Modified Build.

Location	Instrumentation
Core	
Inlet	3 total pressures, 3 static pressures, 3 total temperatures
Preswirl cascade exit	4 static pressures
Vaneless diffuser exit	8 static pressures, 4 traverse locations
Radial deswirl cascade inlet	8 static pressures, 4 traverse locations
Radial deswirl cascade exit	8 static pressures, 4 traverse locations
Sidestream	
Inlet	3 total pressures, 3 static pressures, 3 total temperatures
Plenum	6 static pressures
Guide vane inlet	6 static pressures
Guide vane exit	6 static pressures, 4 traverse locations (same as core deswirl exit)
Stage Exit	4 total pressures, 8 static pressures, 4 total temperatures, 4 traverse locations

bellmouth was open to ambient conditions; the sidestream flow was controlled by restricting the sidestream bellmouth using a combination of cloths and screens. The airflow was determined using total and static pressure measurements at the core bellmouth and sidestream inlet piping. An additional component of the testing was to determine the total temperature mixing that occurred from the sidestream injection location to the stage exit location. To accomplish this, the sidestream inlet was hooked into a heating duct in the laboratory. In this way, temperature differences between the core and sidestream of about 35°F to 40°F were possible.

All data logging was accomplished using a PC-based data acquisition system (DAS) developed by the outside source. Pressure lines from the test rig are routed into the DAS and connected to individual switching solenoids, one solenoid per pressure tap. These solenoids are attached to a "spider" that is connected to the pressure transducers. There are three variable reluctance pressure transducers (low, medium, and high pressure) that are individually calibrated and zeroed out before each set of tests. The diaphragms for these transducers are selected based on the expected pressures in the test rig, and care is taken to select diaphragms that deliver the most accurate readings within the range of likely test pressures. The quoted accuracy for these transducers is 0.25 percent full scale. The calibration accuracy for the testing reported here was 0.19 percent full scale for the low transducer (0.5 ± 0.001 psi), 0.17 percent full scale for the middle transducer (6.0 ± 0.01 psi), and 0.08 percent full scale for the high transducer (13.0 ± 0.01 psi). Thermocouple lines from the test rig are also routed into the DAS. The thermocouples used for this testing were Type E, with a system accuracy of ± 0.8°R. The calibration accuracy for the testing reported here was ± 0.06°R. The three-hole cobra probes that were used for full flow field traversing were also individually calibrated before each set of tests for Mach number effects in the range of expected Mach numbers, and the flow angle null was checked before each test.

THE CFD ANALYSES

Development of the gridding and boundary conditions for a sidestream CFD analysis can be very time consuming. Due to resource and time constraints, the OEM engaged a third party to develop all computational meshes and to complete some of the CFD runs.

This CFD software uses a finite volume method, which solves the three-dimensional Reynolds-averaged Navier-Stokes equations for fluid flow within complex geometries.

Grid Generation

Prior to the construction of the computational grids, the sidestream inlet geometry was divided into three parts. The first part, referred to hereafter as the swirl vane section, included the swirl vane cascade up to the top of the return channel bend. The second part, referred to hereafter as the main section, started at the top of the return channel bend and included the return channel deswirl vanes, the sidestream inlet plenum, the sidestream scoop vanes, and the inlet guidevanes. The third part, referred to hereafter as the nozzle section, included a short section of circular pipe and

the transition nozzle up to the inlet plenum. The grid for each part was constructed separately. All grids used body-fitted, hexahedral elements in a structured multiblock arrangement.

In the interest of reducing the computational model size and complexity, only a single swirl vane out of 23 was included in the swirl vane section grid. This was based on the assumption of an axisymmetric core inlet flow and near axisymmetric flow at the top of the return channel bend. Therefore, the swirl vane section grid effectively included a 1/23rd slice of the swirl vane cascade, thus significantly reducing the size of this portion of the grid. The swirl vane section grid was created using a bladed row grid generation software tool. This grid was used in both the original and modified sidestream inlet analyses.

Two main section grids were created for this project: one each for the original and modified sidestream inlet geometries. In this section, the full 360 degree geometry was modeled. The main section grids were constructed using a multiblock structured mesh generation software, taking advantage of the topology replication feature to reduce the user effort.

The nozzle section grid was also constructed in the multiblock structured mesh generation software. This grid was used in both the original and modified sidestream inlet analyses.

The final grids for the original and modified sidestream inlet analyses combined the three parts: main, swirl vane, and nozzle. The swirl vane section was connected to the main section by way of a circumferential-averaging "stage" interface feature in the CFD software mentioned earlier. The nozzle section was connected to the main section by way of a general grid interface feature in the CFD software, which allows the connection of mismatched grids. The final grids each totaled approximately 800,000 nodes in size.

Physical Properties and Boundary Conditions

The fluid was modeled as air and was assumed to behave as an ideal gas with constant specific heats and molecular viscosity. With a Reynolds number of approximately 10^6, the flow was considered to be turbulent, and the turbulence was modeled by the standard k-epsilon model with standard wall functions.

The boundary conditions were applied as follows:

- *Wall boundaries*—All solid wall boundaries were considered to be aerodynamically smooth, no-slip surfaces.

- *Core inflow boundary*—Prescribed uniform total pressure and temperature. A hub to shroud profile was used to prescribe the flow direction and to align it with the grid as an approximation of the flow streamlines. The flow direction implied zero swirl.

- *Nozzle inflow boundary*—Prescribed uniform total pressure and temperature with a flow direction normal to the inflow boundary plane.

- *Outflow boundary*—Prescribed mass flow rate.

CFD Simulation Procedure

1. A grid representing the entire domain of interest was created.

2. Flow boundary conditions were applied to the grid.

3. Because of the iterative nature of the flow solver, an initial "guess" of the flow solution was required. For the first simulation this was generated as a uniform flow field (velocity, pressure, and temperature.) Subsequent simulations were started from the previous solution.

4. The flow solver was executed to obtain a solution. The first simulation required approximately 30 hours to compute on a four processor CPU with 2 GB RAM. Subsequent simulations required approximately 20 hours to compute.

5. The solution was post-processed with the CFD software to extract quantitative data for comparison to experimental results, and to visualize graphically the flow field.

All postprocessing of the analytical results was done at the OEM's facility. A representative from the third party developed macros to facilitate the interpretation of the results and was present for the initial postprocessing efforts.

OBSERVATION FROM THE TEST AND CFD RESULTS

Operating Conditions

The test conditions that were examined during the testing and duplicated in the CFD analysis are shown in Table 3. Conditions were chosen to examine several sidestream to core mass flow ratios that ranged between 0.25:1 and 1:1. Additional cases involving a heated sidestream flow were also examined. Introduction of flow at different temperatures was primarily intended to create a method to examine mixing in the inlet guidevane (IGV) region.

Table 3. Nominal Test and CFD Operating Conditions.

Case	Nominal Mass Flow Rate Ratio Sidestream:Core Flow	Sidestream Inlet Temperature Relative to Core Flow Inlet [deg. F] (Original Build/Modified Build)
A	0.25:1	+0/+0
B	0.50:1	+0/+0
C	0.75:1	+0/+0
D	1:1	+0/+0
E	0.25:1	+25/+30
F	0.50:1	+25/+30
G	0.75:1	+25/+30
H	1.0:1.0	+25/+30

Several approaches were used to examine the performance of the sidestream design as measured in the test rig and predicted by CFD. A variable area sidestream plenum employed in the modified build was optimized for the 0.50:1 flow case to provide a uniform flow, based on the Mach number in the sidestream plenum. The required circumferential area schedule was based on CFD results from the original build. Performance was assessed through the evaluation of aerodynamic loss and flow uniformity.

Aerodynamic Loss

Aerodynamic losses were examined in the sidestream section, as well as in the mixed flow IGV section. A comparison was made between the test results and the corresponding CFD results. Data were collected for experimental test traverse data, simulated CFD traverse data (same location as physical test traverse), and field averaged CFD results in the associated flow regions. It was realized that accurate analysis of the test data in the nonaxisymmetric sidestream flow field presents a challenge, particularly when only a few discrete locations were examined. In contrast, CFD provides an advantage since results throughout the entire domain can be analyzed; the test data must be used to validate the CFD results before the analytical results can be used with confidence.

Figures 6 and 7 show the normalized loss trends for both the original and modified builds in terms of test measurement and CFD prediction. As might be expected, the comparison between CFD results and experimental measurement is slightly convoluted. Loss comparisons need to be addressed based on the shape of trend lines rather than at an absolute level. The trends in total pressure loss agree reasonably well with the measured traverse data, area averaged CFD, and simulated traverse results.

Agreement between test data and CFD predictions at an absolute level was difficult to assess. In terms of loss comparisons across the various data sources, the reported total pressure loss is highest for the measured traverse data, followed by the CFD area average, and the simulated CFD traverse shows the lowest pressure loss levels. Conversely, the relative loss levels for the various test builds, when compared using the same data source (test data or CFD), show that the losses in modified rig are highest in the sidestream section. The IGV losses did not seem to follow any pattern with regard to the source of data, although the losses predicted by CFD are nearly identical between builds.
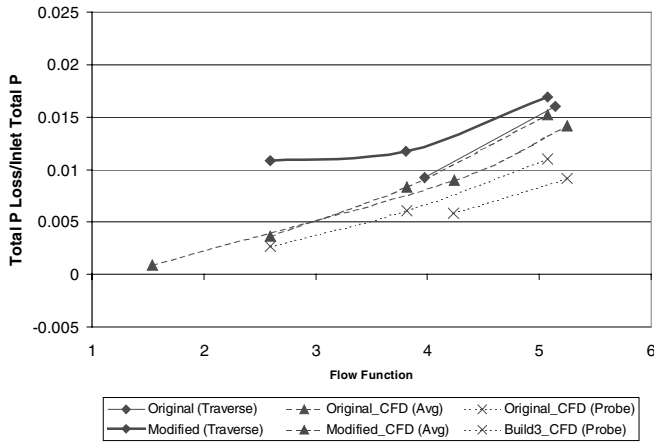
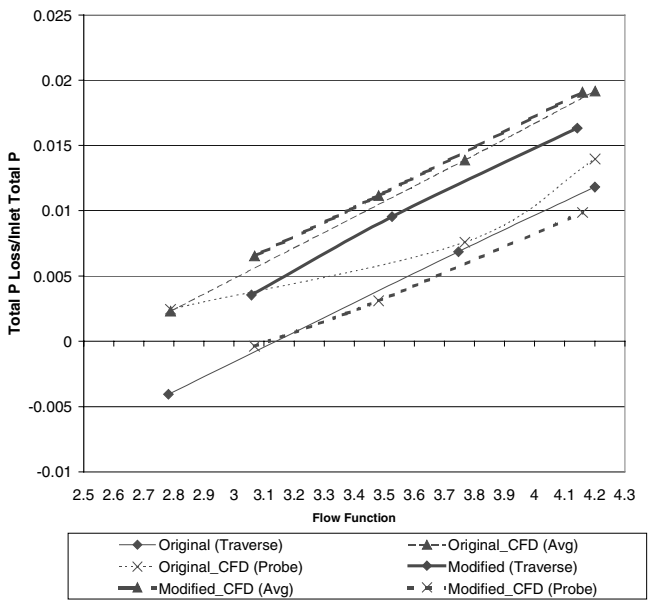*Figure 6. Comparison of Measured and Predicted Sidestream Losses.*

Figure 7. Comparison of Measured and Predicted IGV Losses.

Flow Distribution

In addition to reducing losses, the design changes explored were intended to improve the flow distribution exiting the IGV section, which would ultimately pass into the impeller of the following stage in an actual machine. Test data, flow visualization, and CFD were the tools used to explore flow structure and uniformity throughout the test rig geometry. CFD provides a unique tool to visualize a complex flow at all points in the domain, which is a luxury that is rarely obtained through testing. In an effort to increase the resolution of the empirically observed flow field structure, flow visualization using tufts of yarn attached to the Plexiglas test rig walls and vane surfaces were used to provide a gross indication of flow direction and stability. Flow visualization also assists in qualitative validation of the CFD predictions. Furthermore, flow visualization enhances the quantitative data gathered at the limited number of discrete sampling points available through the installed test probes and flow traverses.

A comparison of the rig exit flow distribution for both builds was studied to determine if any improvements had been made for the limited geometric modifications examined. Figures 8 and 9 present the static pressure distribution in the IGV exit as measured and predicted (the vane numbering system starts at top dead center

at vane zero and progresses in a clockwise fashion, facing the rig from the aft side). Figure 8 examines the highest overall flow in the sidestream model (Case H) with equal flow through the sidestream and core flow sections; Figure 9 shows results for Case F (0.5:1). The CFD predicted average static pressure distribution across the channel falls within the bounds of the static pressure taps located at the hub and shroud. The result supports the use of CFD as a tool in the prediction of flow distribution, at least within the constraints of this study. The ultimate level of accuracy that CFD can achieve is difficult to assess with this data at this time.
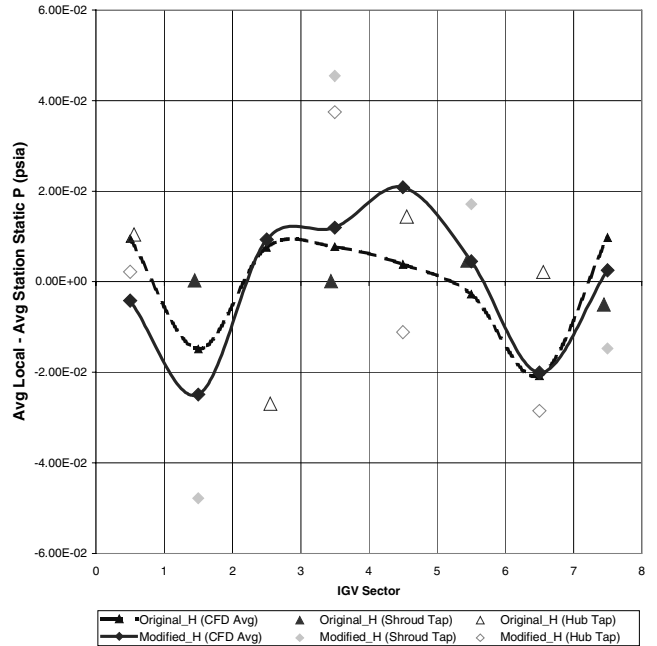

Figure 8. Comparison of Static Pressure Deviation in the IGV Exit Section for the Original and Modified Builds (Case H: Equal Core and Sidestream Mass Flow).
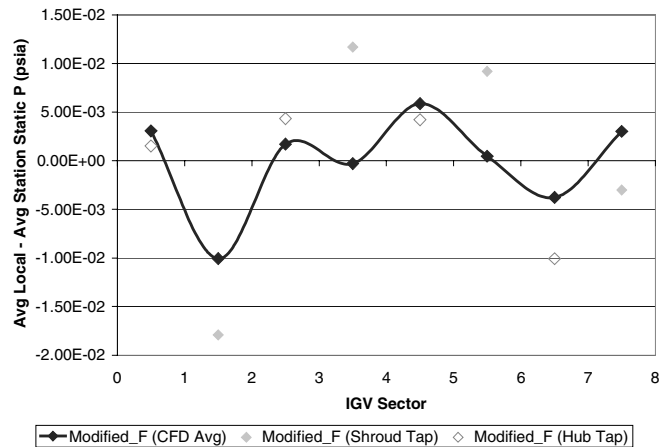

Figure 9. Comparison of Static Pressure Deviation in the IGV Exit Section for the Original and Modified Builds (Case F: Sidestream Mass Flow = 50 Percent Core Flow).

Additional Results—CFD Analysis

Based on the previous discussion, the CFD results appear to support test data and observation in a semiquantitative sense, i.e., trends and rough agreement in parameter values. Therefore some observations relating to the studied design modifications were addressed purely based on CFD results; these observations include

relative component losses within the sidestream elements, flow uniformity in the plenum, and the effectiveness of the sidestream scoop vanes.

The predicted relative loss within the sidestream components (nozzle, plenum, and the vaned sidestream passage) changes somewhat between the original and modified builds. Losses within the plenum and vaned sidestream passage increase in proportion to the nozzle and entry losses predicted in the original build. This redistribution of losses in the sidestream section was attributed mainly to the inclusion of a variable area sidestream plenum.

The flow field predicted by CFD for both the original and modified builds for Case G are shown in Figures 10 and 11. The figures illustrate the Mach number distribution in the plenum and along selected streamtubes. The original build results indicate the existence of larger velocity gradients and low momentum fluid in the plenum region, particularly below the centerline. The modified build presents a flow that might be construed as aesthetically more pleasing; however the results are contrary to the design goals of reduced loss and improved flow uniformity. The variable area plenum was initially based on the hypothesis that the flow uniformity entering the sidestream vane channel would be improved if the flow structure in the plenum was better behaved. Reduction of the plenum cross-sectional area in the circumferential direction was intended to reduce the size of dead flow areas and improve the exit distribution in the IGV section. Results indicate that the flow pattern in the plenum was in fact less tortuous and better behaved, however the flow entering the vaned sidestream channel was actually less uniform. In addition, the local velocities in the plenum were increased and resulted in larger frictional losses.

Figure 11. Mach Number Distribution in Plenum and along Selected Streamtubes for Modified Build Geometry.
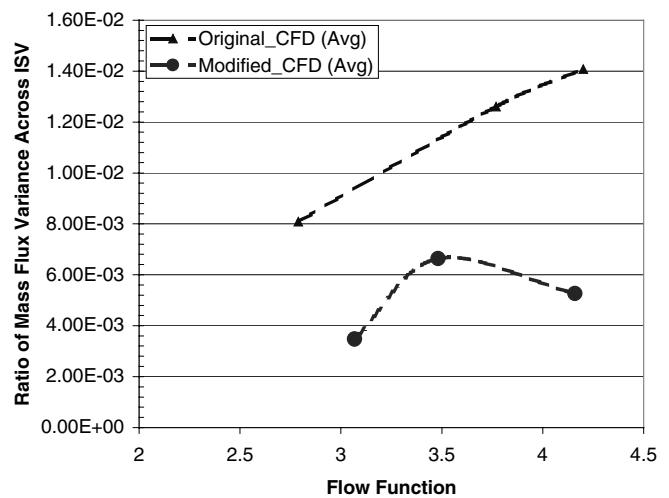
Figure 12. Effectiveness of Sidestream Channel Vanes in Establishing Uniform Flow at IGV Section Inlet.
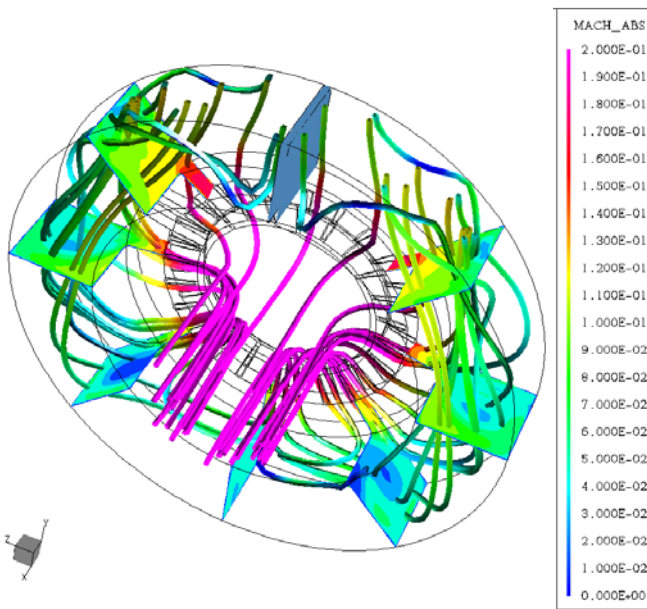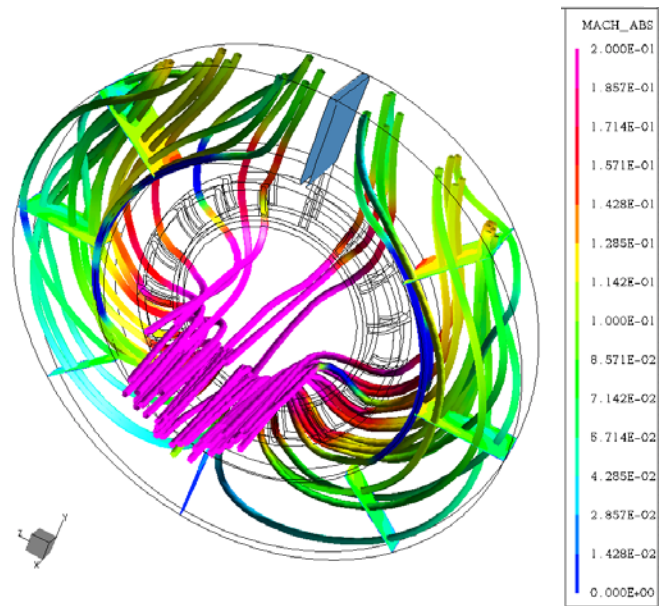

Figure 10. Mach Number Distribution in Plenum and along Selected Streamtubes for Original Build Geometry.

The effectiveness of the sidestream vanes was also evaluated exclusively based on CFD results. The normalized mass flux variations at the inlet of the sidestream vanes and IGVs are shown in Figure 12. Predictions indicate that the flow is less uniform entering the sidestream vane section, most likely due to the variable area sidestream plenum. However, the relative reduction in flow nonuniformity observed in the modified builds indicates that the curved sidestream scoop vanes are more effective than the straight vanes utilized in the original build.

The flow distribution in the exit region is shown in Figures 13 and 14 based on the local Mach number deviation from average for the original and modified builds for flow Case G. The exit flow distribution for the original build appears to be slightly more uniform circumferentially, which was also noted for the other flow cases studied.

RIG RESULTS COMPARED
WITH PRODUCTION SIDESTREAM

As noted in the introduction, there have been attempts to obtain detailed loss data, etc., from sidestreams in production compressors. The majority of these tests included only one or two additional Kiel head total pressure probes at the mixing section or at the inlet guidevane exit (i.e., at the downstream impeller eye). These tests did provide some crude input on the bulk losses in the sidestream plenum or adjacent return channel. However, the limited number of instruments prevented any detailed loss breakdown; i.e., they provided limited understanding regarding the source of the losses.

Occasionally, it was possible (or necessary) to install a sufficient number of instruments to gain insight into the losses associated
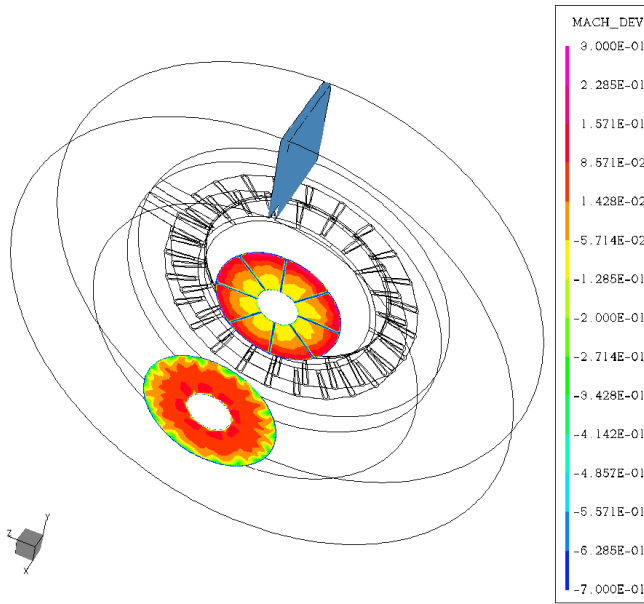
Figure 13. Mach Number Deviations from In-Plane Average Normalized by In-Plane Average Mach Number. Model Exit Plane and IGV Exit Plane Are Shown for the Original Build.
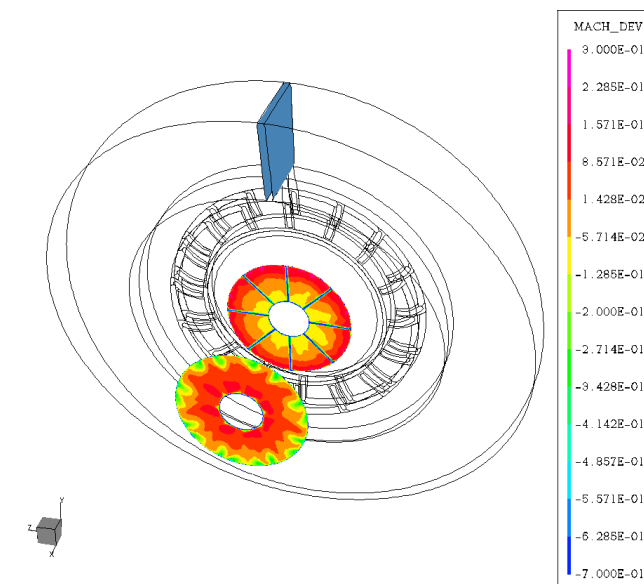

Figure 14. Mach Number Deviations from In-Plane Average Normalized by In-Plane Average Mach Number. Model Exit Plane and IGV Exit Plane Are Shown for the Modified Build.

with the individual sidestream components; i.e., the sidestream plenum and scoop vanes, the upstream return channel, and downstream inlet guidevane (or mixing section). A propane compressor tested at the OEM facilities provides a recent example (Figure 15). The compressor had three incoming sidestreams and, by agreement with the end user and contractor, a fairly extensive amount of instrumentation was installed. Instruments included: total pressure and total temperature rakes at the inlet guidevane exit, combination total pressure and total temperature probes at the upstream return channel entrance, and static and total pressure and total temperature measurements at the sidestream flange.

The compressor was tested at ASME PTC-10 (1965) Class III conditions. Data were gathered across a constant speed line from
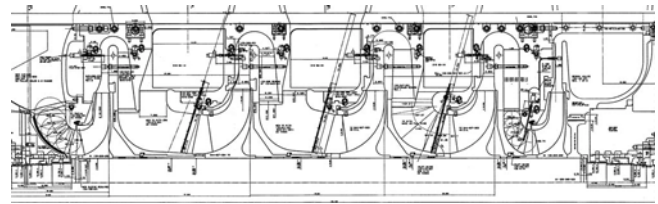

Figure 15. Cross-Section of Production Sidestream Compressor.

near choke flow to near surge. Unlike the development testing described earlier, the ratio of sidestream flow to core flow was maintained near the end user's required sidestream to core flow ratio (1:1) throughout the tests. Of course, the Mach numbers (or velocities) within the core flow path and sidestream passages will increase as the compressor moves from near surge to near overload. Therefore, an assessment of the losses with increased flow was possible.

The end user imposed very tight performance tolerances and some modifications had to be made to the compressor to meet the strict requirements. Therefore, the compressor was tested several times and the detailed sidestream data were collected during each of these tests. Consequently, a tremendous amount of information was gathered for the three sidestreams. The data were assembled into spreadsheets and various plots were generated to assess the variation in sidestream performance with flow rate. Of most interest to the OEM and end user was the variation in pressure drop across the sidestream system with flow; that is, from the return bend upstream of the sidestream to the sidestream inlet flange. Since the sidestreams had different inlet pressures, the ΔP across the sidestream was normalized by the sidestream inlet pressure. The variation in $\Delta P/P$ for one of the three sidestreams is shown in Figure 16. Note that the trends in these data are very similar to those observed in the model test rig and CFD results described earlier (Figure 6). This was not surprising since the model test vehicle was patterned after the sidestream configurations used in the customer unit.
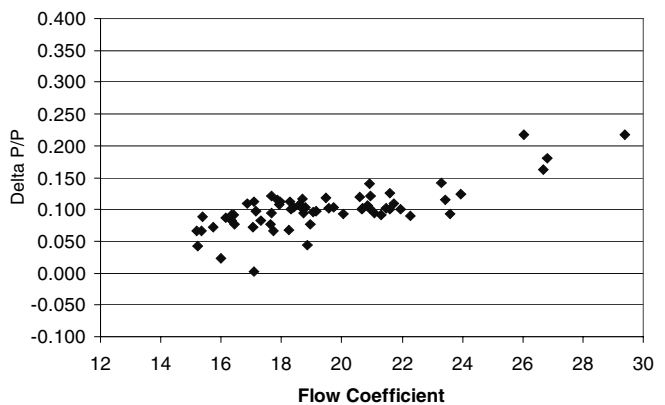

Figure 16. Sidestream Loss Data from a Production Compressor.

In short, the agreement between the production test stand data and model test rig results validated the use of the model rig as a sidestream development tool.

A VIRTUAL TEST RIG

The comparison of the analytical (CFD) and model test results provided fairly good results. The qualitative agreement was quite good. The agreement between CFD and test quantitative measures was also fairly good, though as noted, there were some significant differences between the measured and computed data. Still, the changes in performance predicted by CFD for the two sidestream configurations were quite consistent with the measured difference

from the model testing. In short, CFD showed more promise in assessing the relative changes between two alternate configurations. Based on these results, the analyst can have greater confidence that a design that provides better results in "computational tests" will indeed yield better results in a real machine.

There are many benefits to virtual rig testing in sidestream optimization. However, the most obvious is the potential cost savings to the OEM. As noted previously, sidestreams are most commonly used in very large compressors. Therefore, the costs associated with having to correct an inadequate design are extremely high. Having the ability to computationally "pretest" a new configuration can yield huge savings in the OEM's cost and reputation.

The benefits to the end user are also fairly obvious. If the OEM can use CFD to optimize sidestream configurations, the result will be increased performance and improved predictability. A performance increase results directly in energy savings (i.e., reduced fuel or power consumption) for the end user. More precise predictions of sidestream compressor performance allow process engineers to more accurately establish operating parameters and, therefore, improve production levels. In short, both the OEM and end user benefit from the application of CFD.

The long term benefits of virtual rig testing should also not be overlooked. As has been seen in this work, CFD results can augment performance data gathered on the production test stand to provide a firmer basis for sidestream prediction schemes and loss models. Since full scale testing is typically only possible when doing a customer witness test, the amount of instrumentation that can be installed is limited. However, these data can be used to calibrate the CFD models that in turn can provide the information necessary to establish sound performance models. The result will be even more accurate prediction tools that can be applied to future sidestream applications.

CONCLUSIONS

The sidestream optimization project has shown how a good combination of testing and computational analysis can be used to develop improved design methodologies and prediction schemes. Sidestreams are very complex flow components that historically have been designed via empirical, bulk flow models. While these approaches have served OEM's well in the past, they have a low success rate when challenged by the more demanding requirements of today's end users.

Computational fluid dynamics (CFD) has provided a tool that improved our understanding of the flow physics associated with sidestream flow passages. However, CFD results in and of themselves are not sufficient. The analytical results must be calibrated against quality test data. Such data were acquired as part of this project through model testing. The analytical and test data were compared to assess the viability of the CFD model.

In general, the comparative results were quite promising. The qualitative trends found in the CFD results mimicked those from the model testing. Flow features (i.e., low momentum regions, flow angles, recirculation zones, etc.) seen in the analytical results could also be seen in the flow visualization (i.e., behavior of the tufts).

The quantitative agreement between CFD and measured data was fairly good, especially in the total pressure losses. Also, the calculated performance difference configuration-to-configuration agreed fairly well with the measured difference. However, there were some subtle differences between the analytical and test results, such as details of the loss and static pressure distributions within components. Still, most of these differences can be attributed to the "mass averaged" or "station averaged" nature of the CFD results compared to the "point measurement" nature of the test instrumentation. Therefore, it is concluded that despite the lack of total agreement, CFD can serve as an effective comparative tool in assessing the advantages/disadvantages of design alternatives.

With regard to the specifics of the sidestream design configurations:

● The modified build reduces loss in the sidestream and improves exit flow uniformity, but only over the narrow range for which it was designed. The sidestream plenum area schedule was determined based on a constant circumferential Mach number in the plenum.

● The proportion of overall total pressure loss in the sidestream was predominantly in the sidestream vane section. The modified build did show higher relative plenum losses, likely due to the higher velocities in the reduced area plenum.

● The sidestream vanes did not appear to have a strong effect on the flow or losses. Each case had the same pitch/chord relationship though the vane shape and number did change. It was clear from the CFD and test results that additional studies are required.

Finally, the success of the project described herein was only possible through the cooperative efforts of the research organization, the CFD software developer, and the OEM. Granted, the OEM could have accomplished the task alone, but the cost and time required would have been significantly higher. Clearly, the outsourcing of the select activities brought the project to closure more effectively from a time, cost, and resource basis.

In conclusion, sidestream design remains a difficult task but computational fluid dynamics, supported by quality test data sets, has provided analysts with the tool needed to meet the challenge.

NOMENCLATURE

CFD	=	Computational fluid dynamics
DAS	=	Data acquisition system
IGV	=	Inlet guidevane
Mach-Abs	=	Absolute Mach number
Mach-Dev	=	Mach number deviations from in-plane average normalized by in-plane average Mach number
OEM	=	Original equipment manufacturer
P	=	Pressure (total)
ΔP	=	Change in total pressure

REFERENCES

ASME PTC-10, 1965 (reaffirmed 1979), "Compressors and Exhausters," American Society of Mechanical Engineers, New York, New York.

TASCflow Version 2.9 Users Manual, 1999, AEA Technology/ Advanced Scientific Computing, Waterloo, Ontario, Canada.

BIBLIOGRAPHY

Aungier, R. H., 2000, *Centrifugal Compressors*, New York, New York: ASME Press.

Blahovec, J. F., Matthews, T., and Eads, K. S., 1998, "Guidelines for Specifying and Evaluating New and Rerated Multistage Centrifugal Compressors," *Proceedings of the Twenty-Seventh Turbomachinery Symposium*, Turbomachinery Laboratory, Texas A&M University, College Station, Texas, pp. 215- 231.

Bloch, H. P., 1996, *A Practical Guide to Compressor Technology*, New York, New York: McGraw-Hill.

Sorokes, J. M. and Taylor, R. A., 1992, "Ethylene Plant Centrifugal Compressors—An Overview," Proceedings of the Fourth Annual Ethylene Producers Conference, AIChE, New Orleans, Louisiana.